Experimental Neurology 219 (2009) 404–413

Contents lists available at ScienceDirect

Experimental Neurology

journal homepage: www.elsevier.com/locate/yexnr

Protein ubiquitination in postsynaptic densities after hypoxia in rat neostriatum is blocked by hypothermia

Francisco Capani [a,*,1], Gustavo Ezequiel Saraceno [a,1], Valeria Botti [b], Laura Aon-Bertolino [a], Diêgo Madureira de Oliveira [c], George Barreto [d], Pablo Galeano [a], Lisandro Diego Giraldez-Alvarez [c], Héctor Coirini [b]

[a] Laboratorio de Citoarquitectura y Plasticidad Neuronal, Instituto de Investigaciones Cardiológicas "Prof. Dr. Alberto C. Taquini" (ININCA), UBA-CONICET, Marcelo T. de Alvear 2270, C1122AAJ, Buenos Aires, Argentina
[b] Laboratorio de Neurobiología, Instituto de Biología y Medicina Experimental (IBYME), CONICET, Vuelta de Obligado 2490, C1428ADN, Buenos Aires, Argentina
[c] Laboratório de Neuroquímica e Biologia Celular, Instituto de Ciências da Saúde, Universidade Federal da Bahia (UFBA), Campus do Canela, 40110-100, Salvador, Bahia, Brazil
[d] Instituto Cajal, C.S.I.C., Avenida Doctor Arce 37, E-28002, Madrid, Spain

ARTICLE INFO

Article history:
Received 17 February 2009
Revised 24 May 2009
Accepted 14 June 2009
Available online 23 June 2009

Keywords:
Postsynaptic density
Hypoxia
Neostriatum
Ubiquitin
Hypothermia
Neuroprotection
Perinatal asphyxia

ABSTRACT

Synaptic dysfunction has been associated with neuronal cell death following hypoxia. The lack of knowledge on the mechanisms underlying this dysfunction prompted us to investigate the morphological changes in the postsynaptic densities (PSDs) induced by hypoxia. The results presented here demonstrate that PSDs of the rat neostriatum are highly modified and ubiquitinated 6 months after induction of hypoxia in a model of perinatal asphyxia. Using both two dimensional (2D) and three dimensional (3D) electron microscopic analyses of synapses stained with ethanolic phosphotungstic acid (E-PTA), we observed an increment of PSD thickness dependent on the duration and severity of the hypoxic insult. The PSDs showed clear signs of damage and intense staining for ubiquitin. These morphological and molecular changes were effectively blocked by hypothermia treatment, one of the most effective strategies for hypoxia-induced brain injury available today. Our data suggest that synaptic dysfunction following hypoxia may be caused by long-term misfolding and aggregation of proteins in the PSD.

Introduction

The ubiquitin–proteasome system (UPS) is a protein complex responsible for the degradation of misfolded proteins. Ubiquitination and protein aggregation are important factors in neuronal function and disease (McNaught et al., 2003; Ehlers, 2004; Yi and Ehlers, 2005; DeGracia and Hu, 2007; Ge et al., 2007). Although dysfunction of the UPS and protein aggregation have been implied in neuronal cell death after ischemia (Hu et al., 2000; Mengesdorf et al., 2002; Liu et al., 2006), the mechanisms responsible for neuronal damage after cerebral hypoxia are only beginning to emerge. Several lines of evidence indicate that overactivation of glutamate receptors within synapses might play a role in the damage produced by a hypoxic–ischemic insult (Choi, 1995). Although over-release of glutamate can be seen a few seconds after the hypoxic injury and rapidly returns to the control value, neuronal death can occur several days following the hypoxic episode (Kirino et al., 1984; Van de Berg et al., 2002). Hence, different types of signals may be involved in late neuronal cell death and they could be triggered at the synaptic level.

The pioneering work of Miller et al. (1964) and several other reports (Capani et al., 1997, 2003; Gisselsson et al., 2005; Clark et al., 2008; Webster et al., 2009) demonstrated that hypothermia is an effective treatment for the severe consequences of a hypoxic–ischemic insult.

We have previously demonstrated that neuronal damage in rat neostriatum after hypoxia is associated with a chain of events that includes the over production of excitatory amino acids, nitric oxide and finally an increased release of reactive oxygen species (ROS) (Capani et al., 1997, 2001, 2003). These events are well correlated with behavioral alterations (Loidl et al., 2000).

Electron microscopy observations showed alterations in neuronal subcellular organization like disaggregation of polyribosomes, abnormalities of the Golgi apparatus, edema in the oligodendrocytes and an age-related augmentation in the number of presynaptic boutons in neocortex (Kirino et al., 1984; Petito and Pulsinelli, 1984; Smith et al., 1984; Capani et al., 1997; Martone et al., 1999; Van de Berg et al., 2000; Liu et al., 2005). Recently, changes in postsynaptic density (PSD) thickness (Martone et al., 1999; Liu et al., 2004) and additional dark aggregates throughout the soma and dendrites and PSDs of post-

* Corresponding author. Instituto de Investigaciones Cardiológicas "Prof. Dr. Alberto C. Taquini" (ININCA), UBA-CONICET, Marcelo T. de Alvear 2270, C1122AAJ, Buenos Aires, Argentina. Fax: +5411 4508 3880/8.
E-mail address: fcapani@fmed.uba.ar (F. Capani).
[1] These authors contributed equally to this work.

0014-4886/$ – see front matter © 2009 Elsevier Inc. All rights reserved.
doi:10.1016/j.expneurol.2009.06.007

ischemic dying neurons have been described (Hu et al., 2000; Liu et al., 2004).

Here, we combine two dimensional (2D) and three dimensional (3D) electron microscopy techniques, ethanolic phosphotungstic acid (E-PTA) staining, immunoelectron microscopy and Western blot analysis for ubiquitin to study the morphological and molecular modifications of PSDs in neostriatum 6 months after the induction of hypoxia. We have employed a rat model of perinatal asphyxia (PA), which reproduces clinical situations when umbilical cord circulation is altered. In this model acidosis, hypercapnia and hypoxia are present in the whole body (Lubec et al., 1997; Loidl et al., 2000). Our aims were to determine: (1) how the duration of hypoxia, i.e. the time of asphyxia exposure, correlates with alterations in PSD ultrastructure; (2) whether these changes induce a progressive accumulation of ubiquitin-protein conjugates (ubi-proteins) in PSD; and (3) whether hypothermia (HYP) treatment blocks these alterations. We have demonstrated that PSDs are highly modified and ubiquitinated dependent on the severity of the hypoxic insult. These long-term PSD alterations may be involved in the hypoxia-induced neuronal dysfunctions. In addition, we present strong evidence that hypothermia halts synaptic alterations.

Materials and methods

Animals

A total of 51 pregnant Sprague Dawley rats were obtained from the vivarium of the School of Medicine at the Universidad de Buenos Aires. At day 14 of gestation they were placed in individual cages and maintained in a temperature- (21 ± 2 °C) and humidity- ($65 \pm 5\%$) controlled environment on a 12-h light/dark cycle (lights on at 7 a.m.). The animals had ad libitum access to food (Purina chow) and tap water. One subgroup of animals ($n = 24$) were used as surrogate mothers, another subgroup ($n = 25$) were assigned to PA or PA + HYP procedures, and the remaining ($n = 2$) were the mothers of the control pups. All procedures involving animals were approved by the Institutional Animal Care and Use Committee at the University of Buenos Aires (School of Medicine) and conducted according to principles set forth in the Guide for the Care and Use of Laboratory Animals (NIH Publications No. 80-23, revised 1996). All efforts were made to reduce the number of animals used and to minimize suffering.

Induction of asphyxia

On gestational day 22, 25 full-term pregnant rats were anesthetized and rendered unconscious by CO2 inhalation (Dorfman et al., 2006), rapidly decapitated and the uterus horns were isolated through an abdominal incision and placed in a water bath at 37 °C for 10 min (slight PA; 6 uterus horns from 3 dams), 15 min (moderate PA; 6 uterus horns from 3 dams), 19 min (subsevere PA; 8 uterus horns from 4 dams) and 20 min (severe PA; 24 uterus horns from 12 dams) (Bjelke et al., 1991; Van de Berg et al., 2003). Following the same procedure, other dams ($n = 3$) were hysterectomized and their uterus horns were placed in a bath at 15 °C for 20 min (hypothermia during insult group [HYP 20 min]). In this hypothermia procedure the temperature of the pups is expected to be higher than the one set for the water bath (Engidawork et al., 2001) and, in addition, we and others have previously obtained 100% survival rate with important protective effects using the same protocol (Capani et al., 1997; Loidl et al., 1997, 2000). We chose 20 min as the maximum time of PA because 21 or more minutes of PA results in a survival rate lower than 3% (Bjelke et al., 1991). Following asphyxia, the uterus horns were rapidly opened, the pups were removed, the amniotic fluid was cleaned and the pups were stimulated to breathe by performing tactile intermittent stimulation with pieces of medical wipes for a few minutes until regular breathing was established. The umbilical cord was ligated and the animals were left to recover for 1 h under a heating lamp. When their physiological conditions improved, they were given to surrogate mothers which had delivered normally within the last 24 h. The different groups of pups were marked and mixed with the surrogate mothers' normal litters. We maintained litters of 10 pups with each surrogate mother. The different groups of asphyctic animals was determined based on their different survival rate as described in Capani et al. (1997) and Loidl et al. (2000).

Post-asphyxia procedures

Adult male rats of 6 months of age ($n = 17$–21 animals per group), were anesthetized with 28% (w/v) chloral hydrate, 0.1 ml/100 g of body weight, and perfused with 4% paraformaldehyde in phosphate buffer 0.1 M, pH 7.4 through the abdominal aorta (Gonzalez Aguilar and De Robertis, 1963). Brains were dissected and post-fixed in the same solution for 2 h, and then immersed overnight in phosphate buffer 0.1 M, pH 7.4 containing 5% of sucrose. Coronal brain sections containing the neostriatum (40 μm and 200 μm thick) were cut on an Oxford vibratome and recovered for electron microscopic studies. Some of these sections were stained with cresyl violet according to the procedures described in Capani et al. (1997).

Stereological analysis of calbindin

Striatum was defined according to Paxinos and Watson (1986). Different lines were drawn to define the exact area to be quantified. Medially a line was drawn from the dorsal tip of the left-brain side to the top of the corpus callosum. Dorsal and lateral boundaries were defined by the corpus callosum; a line drawn from the ventral tip of the lateral ventricle to the rhinal fissure was used as a ventral boundary. Laterally a line was drawn from the ventral tip of the lateral ventricle to the corpus callosum. Anterior and posterior boundaries for the striatum were set at bregma 1.6 mm and −0.8 mm. (Schmitz and Hof, 2000).

For estimates of the total number of immunoreactive (IR) calbindin neurons, every 8th section of the brains of control ($n = 4$), PA (10 min [$n = 6$], 15 min [$n = 6$], 19 min [$n = 8$] and 20 min [$n = 8$]), and hypothermia ($n = 8$) treated animals were analyzed using the optical dissector.

The CAST-Grid software (Olympus, Denmark) was used for quantification. The IR neurons, which came into focus within approximately 450 systematically randomly spaced dissectors, were counted at a final magnification of ×3600 (distance between dissectors in mutually orthogonal directions x and y on the sections: 250 μm). The optical dissectors had a base area of 1250 μm^2. Estimated total numbers of IR neurons were calculated from the number of counted neurons and the sampling probability (Schmitz, 1998). Sampling was optimized for prevention of type II error probability due to stereological sampling. The precision of the estimated total numbers of neurons was predicted following Schmitz and Hof (2000).

Electron microscopic studies

Coronal brain sections were cut at a thickness of 200 μm with a vibratome through the level of the dorsal neostriatum and post-fixed for 1 h with 4% paraformaldehyde in 0.1 M cacodylate buffer, pH 7.4. Then tissue sections from hypoxic and control animals were stained either by 1% E-PTA or applying the conventional osmium–uranium–lead method. For conventional osmium–uranium–lead staining, sections were post-fixed for 2 h in 1% osmium tetroxide in 0.1 M cacodylate buffer, rinsed in distilled water, and stained with 1% aqueous uranyl acetate overnight. The sections were then dehydrated in an ascending series of ethanol up to 100%, followed by dry acetone, and embedded in resin (Durcupan ACM, Fluka, Buchs, Switzerland). Thin sections were counterstained with lead citrate before

examination in the electron microscope. For E-PTA staining, sections were dehydrated in an ascending series of ethanol up to 100% and stained for 1 h with 1% PTA. Sections were then embedded in resin (Durcupan ACM, Fluka, Buchs, Switzerland). For conventional electron microscopy we have obtained micrographs from the synapses and the neuronal cell body. For E-PTA staining we have focused on the PSDs since this technique is used mainly to identify postsynaptic densities.

Quantitative analyses of thin sections

Tissue sections were cut at thickness of 100 nm and examined and photographed at 80 keV at a magnification of 8300× with a Zeiss M109 electron microscope (Carl Zeiss Inc, Berlin, Germany). For each animal, five micrographs were obtained from neostriatum. The negatives were digitized into a PC computer. Using an image analyzer software (NIH Image 1.6) PSDs were first manually outlined, and then the maximal thickness, minimum thickness, length, and total area of each PSD were determined. All synapses in which the PSD, intracleft line, and presynaptic grid were clearly visible were chosen for analysis. Samples were analyzed from brains of controls ($n=8$), PA (10 min [$n=8$], 15 min [$n=8$], 19 min [$n=8$], 20 min [$n=8$]), and hypothermia ($n=8$) treated animals. The selection criterion resulted in the analysis of between 40 and 75 PSDs per animal for each neostriatum.

Electron microscopy tomography

Before examination in the electron microscope, 10 nm colloidal gold particles were applied to the E-PTA-stained section (0.5 μm) surface to serve as fiduciary cues for subsequent alignment of images. Then sections were examined by a JEOL 4000EX intermediate high-voltage electron microscope at an accelerating voltage of 400 keV. Data for tomographic reconstructions was acquired using the single-axis tilt method. The micrographs were digitized using a high-resolution 1×1 K CCD camera (Photometrics Inc, Tucson, AZ, USA). The tilt axis was determined, and the images were aligned using fiducial alignment and correlational techniques implemented in the SUPRIM image-processing library (Schroeter and Bretaudiere, 1996). Finally, the volume was reconstructed from the tilt series using R-weighted back-projection implemented in SUPRIM. Final volumes were observed and segmentated using the program ANALYZE (Biomedical Imaging Resource, Mayo Foundation, and Rochester, MN, USA). Additional details of the tomographic method used can be found in articles by Perkins et al. (1997).

Immunohistochemistry

Forty micron sections were used to perform immunohistochemistry in control and hypoxic tissues. Sections were washed and rinsed with PBS and PBS with 0.3% Triton X-100 (PBS-T; pH 7.4). Then sections were incubated overnight at 4 °C with the calbindin-D28 primary antibody (Sigma, St. Louis, MO, USA) at a dilution of 1:10,000 in PBS-T with 3% bovine serum albumin (BSA; Sigma, St. Louis, MO, USA). After washing several times with PBS and PBS-T, the sections were immersed in biotinylated donkey anti-rabbit IgG (1:800; Jackson ImmunoResearch Laboratories, Inc., West Grove, PA, USA) for 2 h at room temperature (RT), followed by ABC-kit detection (1:800; Vectastain, Burlingame, CA, USA). To develop, the sections were pre-incubated for 8 min in 0.3% 3.3′-diaminobenzidine tetrahydrochloride (DAB, Sigma) and stained for 5 min in 0.3% DAB containing 0.03% H_2O_2. Finally the sections were washed and mounted on gelatine-coated slides.

Immunoelectron microscopy

Immunoelectron microscopy was performed on control and post-asphyctic brain tissues using a pre-embedding protocol. Brains were fixed in 4% paraformaldehyde containing 0.1% glutaraldehyde. Brain sections were incubated first with an anti-ubiquitin antibody (Chemicon International, Temecula, CA, USA) overnight (diluted 1:1000 in PBS). Following several wash steps with PBS, neostriatal sections were incubated with biotinylated anti-mouse secondary antibody for 1 h (Amersham), followed by incubation with ABC complex solution (Vectastain ABC kits, Vector Laboratories Inc., Burlingame, CA, USA) for 1 h. After washing in PBS, sections were developed with DAB solution until staining was optimal as examined by light microscopy. Neostriatal sections were post-fixed in 1% osmium tetroxide in 0.1 M cacodylate buffer, rinsed in distilled water, and stained with 1% aqueous uranyl acetate overnight. Tissue sections were dehydrated in an ascending series of ethanol concentrations followed by dry acetone, and embedded in resin (Durcupan ACM, Fluka, Buchs, Switzerland) as above. Sections were cut at a thickness of 0.1 μm and examined with Zeiss M109 electron microscope (Carl Zeiss Inc, Berlin, Germany).

Subcellular fractionation and preparation of PSDs

The crude synaptosomal fraction (P2) was prepared according to the method described previously by Hu and Wieloch (1995) and Liu et al. (2004). Neostriatum tissues were obtained from 5 rats from each group and homogenized with a Dounce homogenizer (25 strokes) in 15 vol of ice-cold homogenization buffer containing 15 mM Tris/HCl pH 7.6, 1 mM DTT, 0.25 M sucrose, 1 mM MgCl2, 1.25 μg/ml pepstatin A, 10 μg/ml leupeptin, 2.5 μg/ml aproptonin, 0.5 mM PMSF, 2.5 mM EDTA, 1 mM EGTA, 0.1 M Na_3VO_4, 50 mM NaF, and 2 mM sodium pyrophosphate. The homogenates were centrifuged at 800 *g* at 4 °C for 10 min, and the supernatants were centrifuged at 10,000 *g* at 4 °C for 15 min to obtain P2. This P2 fraction was loaded onto a sucrose density gradient of 0.85 M/1.0 M/1.2 M and centrifuged at 82,500 *g* for 2 h at 4 °C. The light membrane (LM) fraction was obtained from the 0.85/1.0 sucrose interface, and the synaptosomal fraction was collected from the 1.0 M/1.2 M sucrose interface. After washing with 1% Triton X-100, synaptosomal pellets were collected by centrifugation and then subjected to a second 1.0 M/1.5 M/2.0 M sucrose density gradient centrifugation at 201,000 *g*, 4 °C for 2 h. The isolated PSD fraction was obtained from the 1.5 M/2.0 M interface of the sucrose gradients. The PSD fraction was diluted with an equal volume of 1% Triton X-100/300 mM KCl solution, mixed for 5 min, and centrifuged at 275,000 *g* for 1 h. The PSDs were resuspended in a buffer containing 50 mM Tris/HCl, pH 7.4, 0.5 mM DTT, 100 mM KCl, 10 μg/ml leupeptin, 5 μg/ml pepstatin, 5 μg/ml aprotinin, 0.2 mM phenylmethylsulfonyl fluoride, and 0.2 mM sodium orthovanadate. Then PSDs were dissolved in 0.3% SDS for biochemical analysis.

Western blot

Western blot analysis was carried out using PSD fractions separated on 8% SDS-PAGE (Hu and Wieloch, 1994). Samples containing 20 μg of protein from the control group and experimental groups were applied to each lane. After electrophoresis, proteins were transferred to an Immobilon-P membrane (Amersham). The membranes were incubated with a primary antibody that recognizes free ubiquitin and ubi-proteins (Chemicon International, Temecula, CA, USA, 1:2000) overnight at 4 °C. The membranes were incubated with horseradish peroxidase-conjugated anti-mouse secondary antibody for 45 min at RT. The blots were developed with an ECL detection kit (Amersham). The films were scanned, and the optical density of protein bands was quantified using Kodak 1D gel analysis software.

Statistical analysis

The results were expressed as the means ± standard deviation (SD), unless otherwise noted. Group differences between the means of the IR calbindin neurons, the area of the PSDs, the length of the

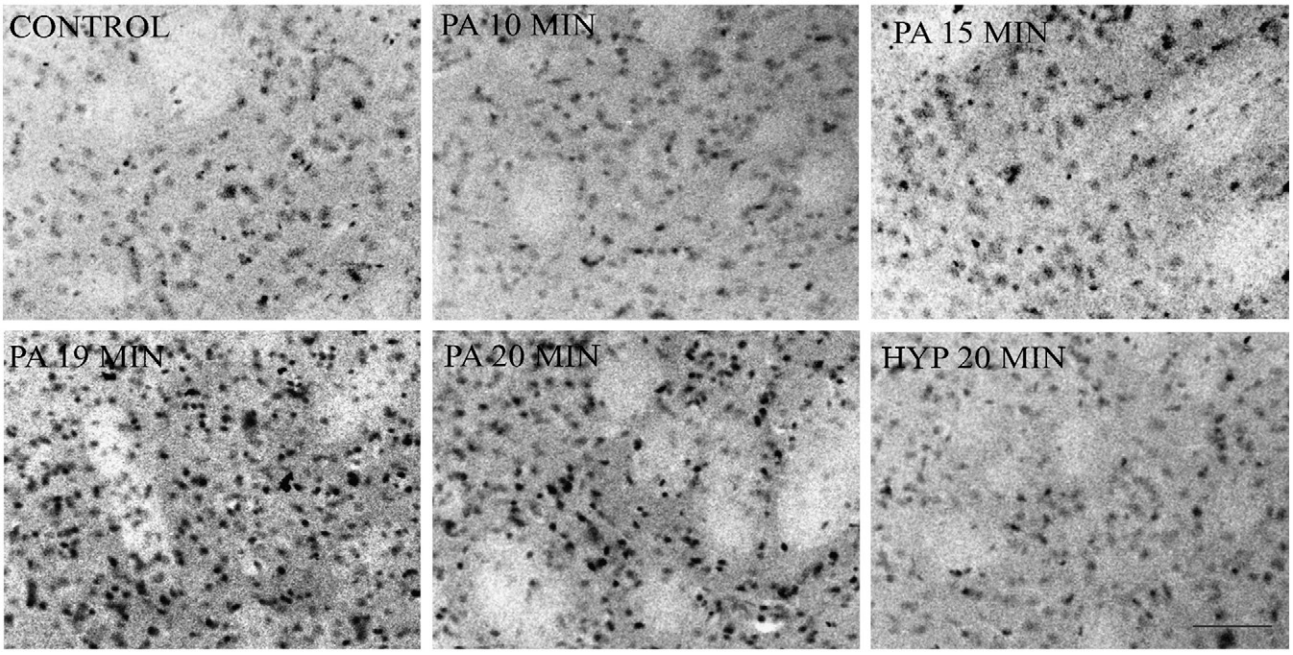

Fig. 1. Low-power micrographs of dorsal neostriatum from 6 month old control rats, rats subjected to different times of PA, and hypothermia-treated rats (HYP 20 min). Vibratome sections of 40 μm were cut and stained with cresyl violet. A clear nuclear condensation was observed after 19 min and 20 min of PA. Hypothermia (HYP 20 min) prevented nuclear condensation. Scale bar, 30 μm.

PSDs, the minimum and maximum thickness of the PSDs and the optical densities of the protein bands from Western Blot analysis were revealed by six one-way ANOVAs. If the overall ANOVA was significant, comparisons between each one of the experimental groups (i.e. PA 10 min, PA 15 min, PA 19 min, PA 20 min and HYP 20 min) and the control group were carried out by two-tailed Dunnett's post hoc test. When the assumption of homogeneity of variances was rejected by Levene's test (this was the case for the optical densities from the Western blot analysis), the overall ANOVA was followed by the multiple comparison Dunnett's T3 post hoc test. Differences with a probability of 5% or less were considered to be significant ($P<0.05$). All the statistical analysis was performed using the SPSS 13.0 for Windows statistical package (SPSS Inc, Chicago, IL).

Results

Microscopic analysis of neostriatal sections

Staining of neostriatal sections with cresyl violet revealed clear nuclear condensation after 6 months in subsevere and severe hypoxic

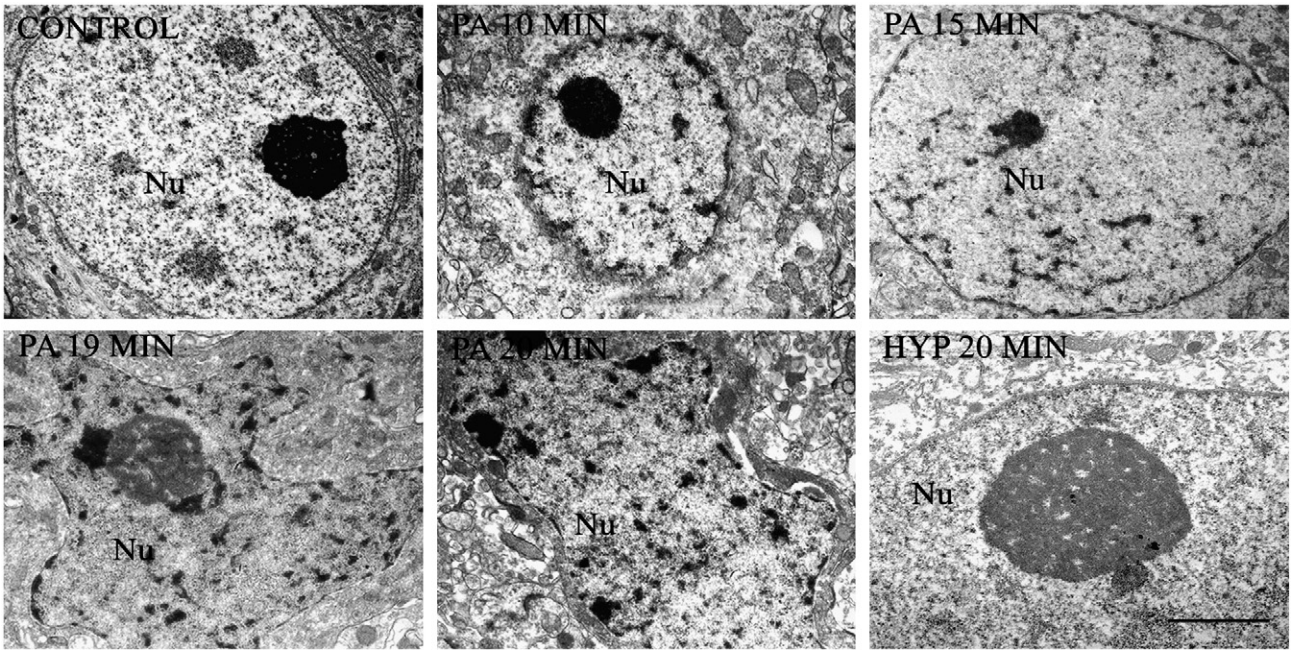

Fig. 2. Ultrastructural organization of the Golgi Type I neuron (GABAergic neuron) in the neostriatum area from 6 month old control rats, rats subjected to different time of PA and hypothermia-treated rats (HYP 20 min). Note that the morphological characteristics of neurodegeneration in asphyctic animals are more pronounced the longer the exposure time of PA was (see text for details). Nu = nucleus. Scale bar, 1 μm.

Table 1
Estimates of the mean total number of calbindin-immunoreactive neurons in the neostriatum.

Groups	Mean calbindin IR neurons	% cell loss
Control	724.25 ± 91.40	
PA 10 min	637.33 ± 87.52	− 12.0%
PA 15 min	630.00 ± 124.6	− 13.0%
PA 19 min	528.75 ± 109.7*	− 26.9%
PA 20 min	506.25 ± 98.80**	− 30.1%
HYP 20 min	714.12 ± 89.63	− 1.4%

Data are expressed as means ± SD. Each experimental group was compared to the control group (see text for statistical details).
* $P<0.05$.
** $P<0.01$.

rats (Fig. 1). Slight nuclear condensation was also observed after 10 and 15 min of PA (Fig. 1). To determine the nature of the condensed cells, a conventional electron microscopy study was performed. We had observed that most of the cells that showed nuclear condensation have morphological characteristics that correspond to neurons in degeneration (i.e. a dark cytoplasm with rare vacuoles, nucleus condensation and compaction, a hypertrophic nucleolus, a nucleus with a festoon shape and a twisted nuclear envelope (Capani et al., 1997; Aggoun-Zouaoui et al., 1998; Liu et al., 2004)). These morphologic characteristics were more pronounced the longer the exposure time of PA was (Fig. 2). These ultrastructural alterations were not observed in hypothermic and control groups (Fig. 2).

Analysis of striatal GABAergic neuronal loss

To quantify the loss of neurons in neostriatum we have employed stereology combined with calbindin immunostaining that identified GABAergic neurons in neostriatum (Van de Berg et al., 2003). We have focused only on GABAergic neurons since they represent the targets of the glutamate synapses from the cortex. The descriptive statistical analysis indicated lower means of calbindin IR neurons, in comparison to control group, the longer the exposure time of PA was. The overall ANOVA was significant ($F_{(5,\ 34)}=5.53$; $P<0.01$) and post hoc tests showed that the decrement of the means of calbindin IR neurons reached statistical significant at 19 and 20 min of PA ($P<0.05$ and $P<0.01$, respectively) while the mean of the HYP 20 min group was not significantly different from the control group (see Table 1).

Modification in neostriatal PSDs stained with E-PTA

No obvious alterations in synapses were observed in the osmium–lead–citrate-stained neostriatal material from 6 month old control and PA rats (Fig. 3). Presynaptic terminals, presynaptic vesicles and ultrastructural organization of PSDs were intact (Fig. 3). In contrast to the material stained with conventional electron microscopy technique, robust changes were apparent in E-PTA-stained PSDs of rats subjected to PA (Fig. 4 and Table 2). Following PA, the thickness of the PSDs increased compared to controls (Figs. 4 and 5 upper panel, and Table 2). There was also a general increment in the amount of E-PTA-stained material in the post-hypoxic PSDs compared to controls. The statistical analysis performed confirmed these observed changes. Overall ANOVAs for the area and length of the PSDs, and for the minimum and maximum thickness of the PSDs were all significant ($F_{(5,\ 42)}=17.34$, $P<0.001$; $F_{(5,\ 42)}=2.63$, $P<0.05$; $F_{(5,\ 42)}=16.48$, $P<0.001$ and $F_{(5,\ 42)}=15.28$, $P<0.001$, respectively). Post hoc tests revealed that the means of the area of the PSDs were significantly bigger, in comparison to the control group, for the PA 15 min, PA 19 min and PA 20 min groups ($P<0.01$; $P<0.001$; $P<0.001$, respectively). The means of the length of the PSDs were significantly larger, in comparison to the control group, only for the maximum time (PA 20 min group) of perinatal asphyxia ($P<0.05$). The post hoc tests also revealed that the means of the minimum and maximum thickness of the PSDs started to significantly increase from 10 min of PA in comparison to the control group (minimum thickness: $P<0.01$ for CLT vs. PA 10 min and $P<0.001$ for CTL vs. PA 15 min, CTL vs. PA 19 min and CTL vs. PA 20 min. Maximum thickness: $P<0.01$ for CLT vs. PA 10 min and $P<0.001$ for CTL vs. PA 15 min, CTL vs. PA 19 min and CTL vs. PA 20 min). The HYP 20 min

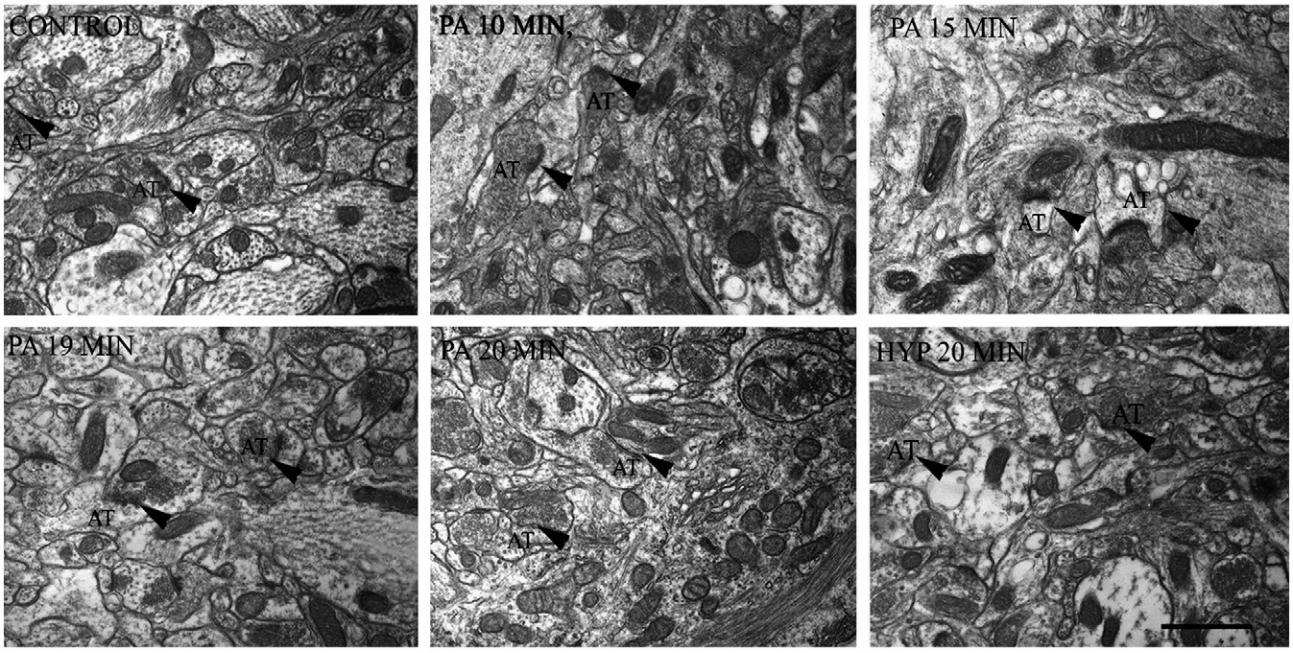

Fig. 3. Electron micrographs of osmium–uranium–lead-stained synapses in dorsal neostriatum from 6 month old control rats, rats subjected to different times of PA and hypothermia-treated rats (HYP 20 min). The synapses (arrowheads) were intact, and no obvious alterations were seen in these osmium–uranium–lead-stained synapses after PA. AT = axon terminal. Scale bar, 0.5 μm.

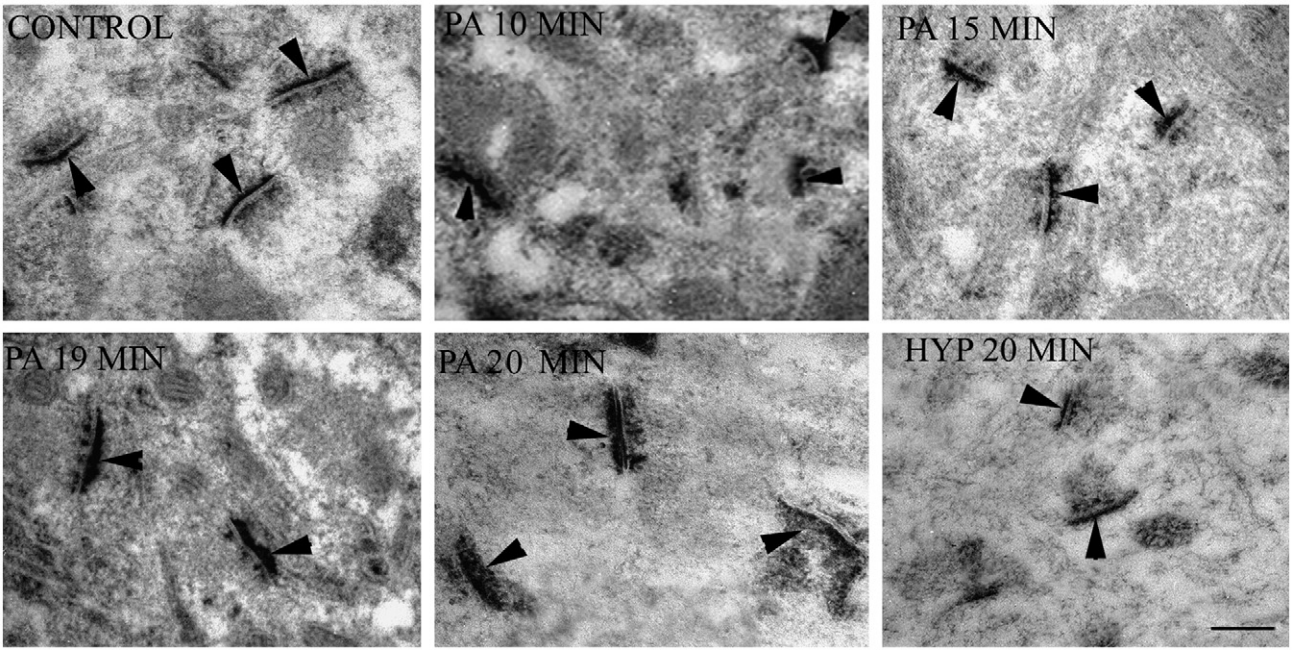

Fig. 4. Electron micrographs of E-PTA-stained PSDs (arrowheads) in neostriatal tissue section from 6 month old control rats, rats subjected to different time of PA and hypothermia-treated rats (HYP 20 min). Note the increased thickness and dispersed appearance of the PSDs in the asphyctic brains, compared with the control. Hypothermic PSDs showed the same thickness as the control. Scale bar, 0.5 μm.

group was not significantly different from the control group for the area of the PSDs, nor for the length of the PSDs, nor for the minimum thickness of the PSDs, nor for the maximum thickness of the PSDs (see Table 2).

The tomographic volumes extended and supported the observations from individual thin sections (Fig. 5, bottom panel). Each volume contained ~2 μm^3 of tissue and between 3 and 8 synapses. Approximately 10 synapses were analyzed for each condition. The density of synapses ranged from 3 to 5-synapses/μm^3, and there was no significant difference in synaptic density between control and post-asphyctic brains indicating that PSD alterations were not attributable to an increase in the number of synapses (data not shown). The PSD volumes were resectioned to produce 2D views similar to those in individual thin sections to correlate 2D and 3D data. Resectioning confirmed the increase in PSD thickness observed in individual thin sections (see Fig. 5, bottom panel). In addition, 3D reconstructions showed that PSDs from post-asphyctic neostriatal synapses were more loosely configured, irregular in shape and more fragmented than those from control brains (Fig 5, bottom panel). At 20 min of PA, neostriatal PSDs showed clear signs of fragmentation and irregular borders in comparison to the control (Fig. 5, bottom panel).

Table 2
Analysis of postsynaptic density features in control, perinatal asphyxia and hypothermia-treated groups.

Groups	Area × 10^3(nm^2)	Length (nm)	Minimum thickness (nm)	Maximum thickness (nm)
Control	2.22 ± 0.63	92.13 ± 11.59	15.21 ± 3.11	41.95 ± 8.75
PA 10 min	3.33 ± 1.00	99.10 ± 13.83	26.04 ± 5.52**	65.50 ± 12.4**
PA 15 min	4.35 ± 0.89**	99.35 ± 11.11	29.57 ± 5.39**	72.04 ± 12.7**
PA 19 min	5.52 ± 1.25**	103.1 ± 12.22	32.61 ± 6.38**	79.11 ± 14.2**
PA 20 min	5.49 ± 1.29**	112.1 ± 12.86*	33.77 ± 7.25**	82.24 ± 16.7**
HYP 20 min	2.38 ± 0.77	93.12 ± 14.30	16.26 ± 5.31	43.40 ± 9.55

Data are expressed as means ± SD. In each variable measured, each experimental group was compared to the control group (see text for statistical details).
* $P<0.05$.
** $P<0.01$.

Ubiquitin-protein conjugates in neostriatal PSDs: immunolabeling and Western blot analysis

Taking advantage of the fact that E-PTA-stained aggregates could be composed of abnormal protein (Martone et al., 1999; Hu et al., 2000), and that ubi-proteins are commonly present in protein aggregates in neurodegenerative diseases (Korhonen and Lindholm, 2004), we performed immunoelectron microscopy for ubiquitin (Fig. 6). Immunolabeling was performed following the procedures previously described by Liu et al. (2004). In control PSDs, ubiquitin was rarely observed (Fig. 6). On the other hand, ubiquitin immunolabeling was more concentrated in PSDs of post-asphyctic 6 month old rats (Fig. 6). Negative controls in which primary antibody was omitted did not show immunolabeling in neostriatal sections (Fig. 6). Western blot analysis confirmed these findings. The isolated PSD fractions were analyzed by immunoblotting with anti-ubiquitin antibody and quantified (Fig. 7). Statistical analysis indicated significant differences between the mean optical densities ($F_{(5,\ 24)} = 58.18$, $P<0.001$). Post hoc tests indicated that the optical densities of the PA 10 min, PA 15 min, PA 19 min and PA 20 min were significantly higher than that of the control group ($P<0.01$ for all comparisons). The mean optical density of the HYP 20 min group was not significantly different from that of the control group ($P>0.05$). As can be seen in Fig. 7, and consistent with results obtained by Liu et al. (2004), most of the ubi-protein bands are between 50 and 250 kDa. However, we also observed additional bands at lower molecular weights. Since free ubiquitin is located in cytosol, and we worked on PSD fraction, those bands could be low molecular weight ubi-proteins.

Effect of hypothermia treatment on PSD morphology

The decrease in temperature from 37 °C to 15 °C markedly reduced nuclear condensation, blocked the neurodegeneration and reduced the thickness of the PSDs (Figs. 1 and 2 and Table 2). 3D electron tomography confirmed these observations (Fig. 5, bottom panel). PSDs from hypothermia animals display an intact ultrastructure similar to the PSDs of the control group. No evident increment in the thickness or alterations in the PSD structure were

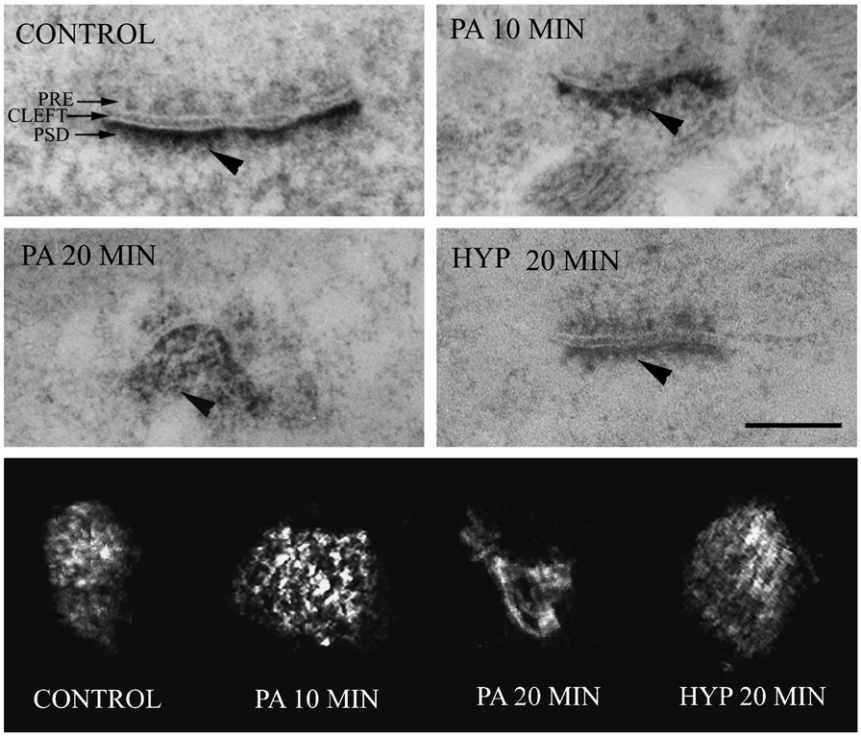

Fig. 5. Upper panel. High-magnification electron micrographs of E-PTA-stained synapses in dorsal neostriatum from 6 month old control rats, rats subjected to different times of PA and hypothermia-treated rats (HYP 20 min). The increment in the thickness is observed at 10 min and reached the maximum at 20 min of PA (arrowheads). Hypothermia PSD did not show aggregation of material. Scale bar, 0.1 μm. PRE, presynaptic specialization; CLEFT, synaptic cleft. **Bottom panel**. 3D images of E-PTA-stained PSDs from tomographic volumes of 6 month old control rats, rats subjected to 10 min or 20 min of PA, and hypothermia-treated rats (HYP 20 min) in dorsal neostriatum. Each PSD was rotated individually to appear in face to be correlated with single 2D images. The contrast is reversed so that stained PSDs appear bright relative to unstained structures. The control PSDs was compact. At 10 min of reperfusion the PSDs appeared thicker. Loosening PSDs with signs of disintegration could be observed at 20 min of reperfusion. Hypothermia showed the same thickness of the control. Scale bar, 0.1 μm.

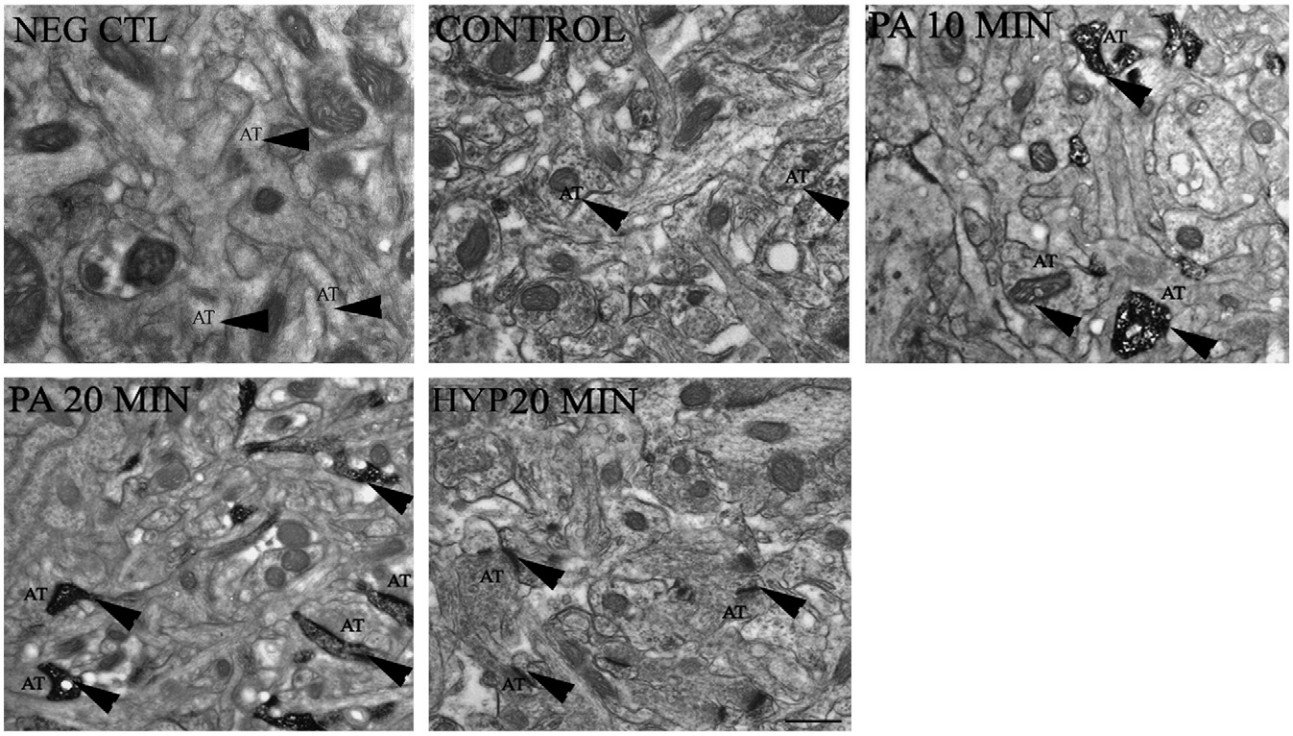

Fig. 6. Electron micrographs of ubiquitin immunolabeling from neostriatal tissue of 6 month old control rats, rats subjected to 10 or 20 min of PA, and hypothermia-treated rats (HYP 20 min). Strong ubiquitin stained was observed in asphyctic PSDs starting at 10 min (arrowheads). In control and hypothermia-treated animals the ubiquitin staining was very weak and rare. The primary antibody omission shows the specificity of the immunostaining (NEG CTL). AT = axon terminal. Scale bar, 0.5 μm.

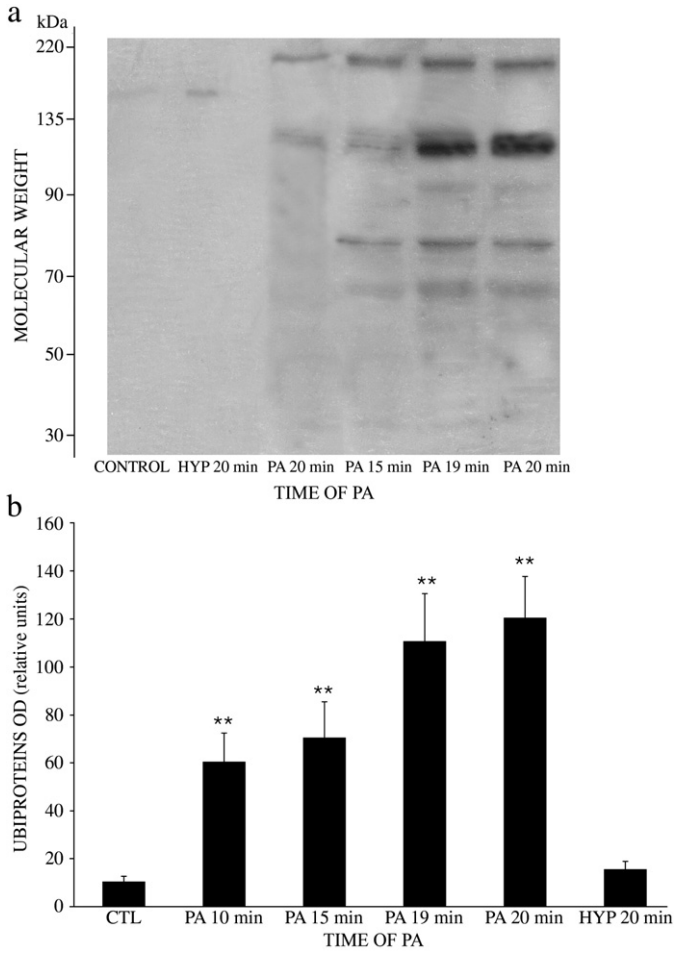

Fig. 7. (a) Immunoblots of ubi-proteins in neostriatal PSDs of 6 month old control rats, rats subjected to different times of PA and hypothermia-treated rats (HYP 20 min). The blots were labeled with the anti-ubi-protein antibody and visualized with an ECL system. The molecular size is indicated at the left. Ubi-proteins are present after PA. HYP 20 min prevented the ubi-proteins formation. A mouse anti-actin monoclonal antibody was used as an internal loading control. (b) Quantification of ubi-proteins on PSDs. Optical density of immunoblot bands are expressed as mean ± SD. $^{**}P<0.01$, between control and experimental groups. PSD = postsynaptic densities; ubi-proteins = ubiquitinated proteins.

seen after hypothermia treatment. Ubi-proteins were hardly detected in control and hypothermic PSDs (Figs. 6 and 7). These data demonstrate that hypothermia counteracts the degeneration of the PDSs affected by PA.

Discussion

In the present report, we demonstrated significant modification in the morphology of PSDs of the neostriatum of 6 month old rats subjected to different periods of hypoxia. The use of electron tomography combined with E-PTA staining clearly showed that ultrastructural alterations were more pronounced in PSDs that were exposed to longer periods of hypoxia (19 and 20 min). Ultrastructural changes of PSDs were strongly correlated with the level of ubiquitin labeling, suggesting that postsynaptic structures are a relevant target for protein ubiquitination following a hypoxic insult. Since ubiquitin primarily tags damaged or unfolded proteins, the increased ubiquitination may be seen as a measure of increased protein damage in the hypoxic PSDs of the neostriatum. Using hypothermia we were able to block these changes completely. These results are consistent with previous reports in different models of ischemia in hippocampus and neocortex (Martone et al., 1999; Hu et al., 2000; Liu et al., 2005), suggesting that PSD protein ubiquitination may be a hallmark of the damage induced in different areas sensitive to hypoxic–ischemic episodes and may be useful as a measure for the severity of the damage induced by the hypoxic insult.

Significance of the ubiquitin conjugated protein accumulation

In agreement with previous studies in other areas of the CNS and different models of ischemia (Martone et al., 1999; Hu et al., 2000; Liu et al., 2005), we did not observe noticeable changes in the PSDs of control and hypoxic groups stained with osmium-heavy metals. However, there was a marked increment in E-PTA-stained material in the 6 month old post-asphyctic PSDs. Although PSD thickness augmentation was evident in slight and moderate PA rats, the most robust alterations were observed following 19 and 20 min of PA, suggesting that the degree of changes at the level of the PSDs is directly correlated with the severity of the PA insult. Tomographic data from 20 min of PA revealed that the PSDs develop very irregular shapes and signs of serious damage. Since the cortical-neostriatal glutamatergic afferent connections represent 80% of the synapses in the neostriatum and due to their asymmetric nature our results provide strong evidence that this specific class of synapse is affected. We did not analyze whether other types of synapses were as well. This question is currently under investigation because the dopaminergic synapses represent the remaining 20% of the total synapses in neostriatum. Dopamine has been implied in neuronal cell death during ischemic and hypoxic episodes before (Wieloch et al., 1990; Nishino et al., 2000; Mitchell and Snyder-Keller, 2003).

The developing brain is very susceptible to alterations generated by the lack of oxygen in spite of its enhanced capacity for brain plasticity (Johnston et al., 2002; Johnston, 2004). Perinatal asphyxia causes neuronal death in the CNS (Capani et al., 1997; Van de Berg et al., 2002) and could induce alterations in synaptic plasticity. Consistent with these results our data demonstrate that at six months after the injury, asphyctic animals show a significant loss of GABAergic neurons, clear signs of neurodegeneration and ubiquitinization of PSDs (see Table 1 and Figs. 1, 2 and 6). It remains to be proven that the ubi-conjugated are one of the causes of the long-term loss in neurons in the neostriatum. However, supporting evidence for this hypothesis was provided in several other studies. The UPS has been implied, for instance, in the process of Wallerian degeneration (Ehlers, 2004). Treatment with inhibitors of the proteosome or when ubiquitination was prevented, allows transected axon to persist in good health for at least 16 h (Ehlers, 2004). Several studies have demonstrated the accumulation of ubiquitin-protein conjugates after brain ischemia in hippocampal neurons (Li and Farooque, 1996; Hu et al., 2000; Liu et al., 2005, 2006) suggesting that an increase in ubi-protein conjugates causes cellular damage. Because GABAergic neurons receive most of the glutamatergic input, these alterations might result in toxic signals, e.g. increased calcium influx propagating to the dendritic shaft and eventually the cell body, causing cell degeneration (Choi, 1995). Calcium influx may induce intracellular proteases such as calpain and possibly some ubiquitin regulatory enzymes inducing the degradation of axonal microtubules and neurofilaments (Garcia and Cleveland, 2001). In addition, calcium mediates the activation of ROS production after hypoxic–ischemic insult inducing further protein damage (Kraig and Wagner, 1987; Capani et al., 2001, 2003; Dingman et al., 2006). Finally, if the hypoxic factor is not counteracted against in time, the overloaded ubiquitin/ATP-dependent pathway might reduce neuronal survival, because damaged proteins are not degraded and accumulate, ultimately leading to irreversible cell damage (Korhonen and Lindholm, 2004). Consistent with this view, Sinigaglia-Coimbra et al. (2002) have reported an increment of ubiquitination after 6 months of transient ischemia combined with hyperthermia. On the other hand, induction of heat shock proteins (HSPs) protects neurons against ischemic insults (Yenari et al., 1998; Sharp et al., 1999; Lee et al., 2001; van der Weerd et al., 2005). Hu et al. (1998) have reported

translocation of both HSC70 and NSF into PSDs after ischemia. These proteins are chaperones destined to prevent protein aggregation. Since degradation of ubi-protein requires the presence of molecular chaperones (Imai et al., 2003; Truettner et al., 2009) the malfunctioning of this system could result in PSD damage by accumulation of ubi-proteins.

In addition, we are inducing hypoxia in rat pups whose synapses are still in development (Fiala et al., 1998). Then, it is also reasonable to think that the hypoxic–ischemic insult could generate early abnormal formation of synaptic contacts that might induce long-term synaptic alterations, ubiquitinization and a saturation of the ubiquitin–proteasome system (UPS) leading to neurological deficits as a consequence of the deposition of ubi-proteins in PSDs (Hu et al., 2000).

PSD alterations and hypothermia treatment prevention

Hypothermia has been shown to provide full protection against cell death during PA and ischemia (Capani et al., 1997) including the recovery phase following the ischemic insult (Coimbra and Wieloch, 1994). Recently Gisselsson et al. (2005) have shown in an in vitro ischemia model that mild hypothermia affects the depolymerization–repolymerization cycle diminishing spine motility and length. These changes may alter protein–protein interactions and induce disruption of the glutamate-NMDA receptor signaling diminishing Ca++ influx that would help to break the chain of events that lead to protein aggregation and cell death. Consistent with this view, Aarts et al. (2002) have shown in vivo and in vitro ischemia models that alterations in NMDA-PSD95 interactions reduce cell death. Recently Liu et al. (2006) reported that hypothermia maintains the concentration of free ubiquitin by blocking the increase of ubiquitin observed after ischemia.

Conclusions

Overall, our data suggest that excessive protein ubiquitination in 6 month old neostriatal post-asphyctic PSDs correlates with the time of exposure to PA, and may be useful as a marker for the grade of alteration of the PSDs and neuronal damage. Hypothermia prevents overproduction of ubi-protein conjugates, thereby providing effective protection against PA damage.

Acknowledgments

This work was supported by Agencia Nacional de Promoción Científica y Técnica (ANPCyT BID 1728/OC-AR PICT 15001), PRODOC/FAPESB 016/2004, FAPESB/CNPq 159/2003, and University of Buenos Aires grants M047 and M020. G. E. Saraceno, L. Aon-Bertolino and P. Galeano are supported by CONICET fellowships. The authors thank National Center for Electron Microscopy and Imaging Research (NCMIR, Neuroscience Department, CA, USA) for its assistance in the tomographic reconstruction data. We thank Jorge Joaquín Llambías for help with English revision. Finally we also thank Ernesto Restrepo and Prof. Dr. Kristen Kristenson (Karolinska Institutet) for the donation of the microscope that made some of the experiments in our laboratory located in Buenos Aires possible.

References

Aarts, M., Liu, Y., Liu, L., Besshoh, S., Arundine, M., Gurd, J.W., Wang, Y.T., Salter, M.W., Tymianski, M., 2002. Treatment of ischemic brain damage by perturbing NMDA receptor–PSD-95 protein interactions. Science 298, 846–850.

Aggoun-Zouaoui, D., Margalli, I., Borrega, F., Represa, A., Plotkine, M., Ben-Ari, Y., Charriaut-Marlangue, C., 1998. Ultrastructural morphology of neuronal death following reversible focal ischemia in the rat. Apoptosis 3, 133–141.

Bjelke, B., Andersson, K., Ogren, S.O., Bolme, P., 1991. Asphyctic lesion: proliferation of tyrosine hydroxylase-immunoreactive nerve cell bodies in the rat substantia nigra and functional changes in dopamine neurotransmission. Brain Res. 543, 1–9.

Capani, F., Loidl, F., Lopez-Costa, J.J., Selvin-Testa, A., Saavedra, J.P., 1997. Ultrastructural changes in nitric oxide synthase immunoreactivity in the brain of rats subjected to perinatal asphyxia: neuroprotective effects of cold treatment. Brain Res. 775, 11–23.

Capani, F., Loidl, C.F., Aguirre, F., Piehl, L., Facorro, G., Hager, A., De Paoli, T., Farach, H., Pecci-Saavedra, J., 2001. Changes in reactive oxygen species (ROS) production in rat brain during global perinatal asphyxia: an ESR study. Brain Res. 914, 204–207.

Capani, F., Loidl, C.F., Piehl, L.L., Facorro, G., De Paoli, T., Hager, A., 2003. Long term production of reactive oxygen species during perinatal asphyxia in the rat central nervous system: effects of hypothermia. Int. J. Neurosci. 113, 641–654.

Choi, D.W., 1995. Calcium: still center-stage in hypoxic–ischemic neuronal death. Trends Neurosci. 18, 58–60.

Clark, D.L., Penner, M., Orellana-Jordan, I.M., Colbourne, F., 2008. Comparison of 12, 24 and 48 h of systemic hypothermia on outcome after permanent focal ischemia in rat. Exp. Neurol. 212, 386–392.

Coimbra, C., Wieloch, T., 1994. Moderate hypothermia mitigates neuronal damage in the rat brain when initiated several hours following transient cerebral ischemia. Acta Neuropathol. 87, 325–331.

DeGracia, D.J., Hu, B.R., 2007. Irreversible translation arrest in the reperfused brain. J. Cereb. Blood Flow Metab. 27, 875–893.

Dingman, A., Lee, S.Y., Derugin, N., Wendland, M.F., Vexler, Z.S., 2006. Aminoguanidine inhibits caspase-3 and calpain activation without affecting microglial activation following neonatal transient cerebral ischemia. J. Neurochem. 96, 1467–1479.

Dorfman, V.B., Vega, M.C., Coirini, H., 2006. Age-related changes of the GABA-B receptor in the lumbar spinal cord of male rats and penile erection. Life Sci. 78, 1529–1534.

Ehlers, M.D., 2004. Deconstructing the axon: Wallerian degeneration and the ubiquitin–proteasome system. Trends Neurosci. 27, 3–6.

Engidawork, E., Loidl, F., Chen, Y., Kohlhauser, C., Stoeckler, S., Dell'Anna, E., Lubec, B., Lubec, G., Goiny, M., Gross, J., Andersson, K., Herrera-Marschitz, M., 2001. Comparison between hypothermia and glutamate antagonism treatments on the immediate outcome of perinatal asphyxia. Exp. Brain Res. 138, 375–383.

Fiala, J.C., Feinberg, M., Popov, V., Harris, K.M., 1998. Synaptogenesis via dendritic filopodia in developing hippocampal area CA1. J. Neurosci. 18, 8900–8911.

Garcia, M.L., Cleveland, D.W., 2001. Going new places using an old MAP: tau, microtubules and human neurodegenerative disease. Curr. Opin. Cell Biol. 13, 41–48.

Ge, P., Luo, Y., Liu, C.L., Hu, B., 2007. Protein aggregation and proteasome dysfunction after brain ischemia. Stroke 38, 3230–3236.

Gisselsson, L.L., Matus, A., Wieloch, T., 2005. Actin redistribution underlies the sparing effect of mild hypothermia on dendritic spine morphology after in vitro ischemia. J. Cereb. Blood Flow Metab. 25, 1346–1355.

Gonzalez Aguilar, F., De Robertis, E., 1963. A formalin-perfusion fixation method for histophysiological study of the central nervous system with the electron microscope. Neurology 13, 758–771.

Hu, B.R., Wieloch, T., 1994. Tyrosine phosphorylation and activation of mitogen-activated protein kinase in the rat brain following transient cerebral ischemia. J. Neurochem. 62, 1357–1367.

Hu, B.R., Wieloch, T., 1995. Persistent translocation of Ca2+/calmodulin-dependent protein kinase II to synaptic junctions in the vulnerable hippocampal CA1 region following transient ischemia. J. Neurochem. 64, 277–284.

Hu, B.R., Park, M., Martone, M.E., Fischer, W.H., Ellisman, M.H., Zivin, J.A., 1998. Assembly of proteins to postsynaptic densities after transient cerebral ischemia. J. Neurosci. 18, 625–633.

Hu, B.R., Martone, M.E., Jones, Y.Z., Liu, C.L., 2000. Protein aggregation after transient cerebral ischemia. J. Neurosci. 20, 3191–3199.

Imai, J., Yashiroda, H., Maruya, M., Yahara, I., Tanaka, K., 2003. Proteasomes and molecular chaperones: cellular machinery responsible for folding and destruction of unfolded proteins. Cell Cycle 2, 585–590.

Johnston, M.V., Nakajima, W., Hagberg, H., 2002. Mechanisms of hypoxic- neurodegeneration in the developing brain. The Neuroscientist 8, 212–220.

Johnston, M.V., 2004. Clinical disorders of brain plasticity. Brain Dev. 26, 73–80.

Kirino, T., Tamura, A., Sano, K., 1984. Delayed neuronal death in the rat hippocampus following transient forebrain ischemia. Acta Neuropathol. 64, 139–147.

Korhonen, L., Lindholm, D., 2004. The ubiquitin proteasome system in synaptic and axonal degeneration: a new twist to an old cycle. J. Cell Biol. 165, 27–30.

Kraig, R.P., Wagner, R.J., 1987. Acid-induced changes of brain protein buffering. Brain Res. 410, 390–394.

Lee, J.E., Yenari, M.A., Sun, G.H., Xu, L., Emond, M.R., Cheng, D., Steinberg, G.K., Giffard, R.G., 2001. Differential neuroprotection from human heat shock protein 70 overexpression in in vitro and in vivo models of ischemia and ischemia-like conditions. Exp. Neurol. 170, 129–139.

Li, G.L., Farooque, M., 1996. Expression of ubiquitin-like immunoreactivity in axons after compression trauma to rat spinal cord. Acta Neuropathol. 91, 155–160.

Liu, C.L., Martone, M.E., Hu, B.R., 2004. Protein ubiquitination in postsynaptic densities after transient cerebral ischemia. J. Cereb. Blood Flow Metab. 24, 1219–1225.

Liu, C.L., Ge, P., Zhang, F., Hu, B.R., 2005. Co-translational protein aggregation after transient cerebral ischemia. Neuroscience 134, 1273–1284.

Liu, J.J., Zhao, H., Sung, J.H., Sun, G.H., Steinberg, G.K., 2006. Hypothermia blocks ischemic changes in ubiquitin distribution and levels following stroke. Neuroreport 17, 1691–1695.

Loidl, C.F., Capani, F., López-Costa, J.J., Selvín-Testa, A., López, E.M., Pecci-Saavedra, J., 1997. Long term changes in NADPH-diaphorase reactivity in striatal and cortical neurons following experimental perinatal asphyxia: neuroprotective effects of hypothermia. Int. J. Neurosci. 89, 1–14.

Loidl, C.F., Gavilanes, A.W., Van Dijk, E.H., Vreuls, W., Blokland, A., Vles, J.S., Steinbusch, H.W., Blanco, C.E., 2000. Effects of hypothermia and gender on survival and behavior after perinatal asphyxia in rats. Physiol. Behav. 68, 263–269.

Lubec, B., Dell'Anna, E., Fang-Kircher, S., Marx, M., Herrera-Marschitz, M., Lubec, G., 1997. Decrease of brain protein kinase C, protein kinase A, and cyclin-dependent kinase correlating with pH precedes neuronal death in neonatal asphyxia. J. Investig. Med. 45, 284–294.

Martone, M.E., Jones, Y.Z., Young, S.J., Ellisman, M.H., Zivin, J.A., Hu, B.R., 1999. Modification of postsynaptic densities after transient cerebral ischemia: a quantitative and three-dimensional ultrastructural study. J. Neurosci. 19, 1988–1997.

McNaught, K.S., Belizaire, R., Isacson, O., Jenner, P., Olanow, C.W., 2003. Altered proteasomal function in sporadic Parkinson's disease. Exp. Neurol. 179, 38–46.

Mengesdorf, T., Jensen, P.H., Mies, G., Aufenberg, C., Paschen, W., 2002. Down-regulation of parkin protein in transient focal cerebral ischemia: a link between stroke and degenerative disease? Proc. Natl. Acad. Sci. U. S. A. 99, 15042–15047.

Miller, J.A., Miller, F.S., Westin, B., 1964. Hypothermia in the treatment of asphyxia neonatorum. Biol. Neonat. 6, 148–163.

Mitchell, E.S., Snyder-Keller, A., 2003. Blockade of D1 dopaminergic transmission alleviates c-*fos* induction and cleaved caspase-3 expression in the brains of rat pups exposed to prenatal cocaine or perinatal asphyxia. Exp. Neurol. 182, 64–74.

Nishino, H., Hida, H., Kumazaki, M., Shimano, Y., Nakajima, K., Shimizu, H., Ooiwa, T., Baba, H., 2000. The striatum is the most vulnerable region in the brain to mitochondrial energy compromise: a hypothesis to explain its specific vulnerability. J. Neurotrauma 17, 251–260.

Paxinos, G.P., Watson, C., 1986. The Rat Brain Stereotaxic Coordinates. Academic Press, Sydney.

Perkins, G.A., Renken, C.W., Song, J.Y., Frey, T.G., Young, S.J., Lamont, S., Martone, M.E., Lindsey, S., Ellisman, M.H., 1997. Electron tomography of large, multicomponent biological structures. J. Struct. Biol. 120, 219–227.

Petito, C.K., Pulsinelli, W.A., 1984. Sequential development of reversible and irreversible neuronal damage following cerebral ischemia. J. Neuropathol. Exp. Neurol. 43, 141–153.

Schmitz, C., 1998. Variation of fractionator estimates and its prediction. Anat. Embryol. (Berl.) 198, 371–397.

Schmitz, C., Hof, P.R., 2000. Recommendations for straightforward and rigorous methods of counting neurons based on a computer simulation approach. J. Chem. Neuroanat. 20, 93–114.

Schroeter, J.P., Bretaudiere, J.P., 1996. SUPRIM: easily modified image processing software. J. Struct. Biol. 116, 131–137.

Sharp, F.R., Massa, S.M., Swanson, R.A., 1999. Heat-shock protein protection. Trends Neurosci. 22, 97–99.

Sinigaglia-Coimbra, R., Cavalheiro, E.A., Coimbra, C.G., 2002. Postischemic hyperthermia induces Alzheimer-like pathology in the rat brain. Acta Neuropathol. 103, 444–452.

Smith, M.L., Bendek, G., Dahlgren, N., Rosén, I., Wieloch, T., Siesjö, B.K., 1984. Models for studying long-term recovery following forebrain ischemia in the rat. 2. A 2-vessel occlusion model. Acta Neurol. Scand. 69, 385–401.

Truettner, J.S., Hu, K., Liu, C.L., Dietrich, W.D., Hu, B., 2009. Subcellular stress response and induction of molecular chaperones and folding proteins after transient global ischemia in rats. Brain Res. 1249, 9–18.

Van de Berg, W.D., Blokland, A., Cuello, A.C., Schmitz, C., Vreuls, W., Steinbusch, H.W., Blanco, C.E., 2000. Perinatal asphyxia results in changes in presynaptic bouton number in striatum and cerebral cortex—a stereological and behavioral analysis. J. Chem. Neuroanat. 20, 71–82.

Van de Berg, W.D., Schmitz, C., Steinbusch, H.W., Blanco, C.E., 2002. Perinatal asphyxia induced neuronal loss by apoptosis in the neonatal rat striatum: a combined TUNEL and stereological study. Exp. Neurol. 174, 29–36.

Van de Berg, W.D., Kwaijtaal, M., de Louw, A.J., Lissone, N.P., Schmitz, C., Faull, R.L., Blokland, A., Blanco, C.E., Steinbusch, H.W., 2003. Impact of perinatal asphyxia on the GABAergic and locomotor system. Neuroscience 117, 83–96.

van der Weerd, L., Lythgoe, M.F., Badin, R.A., Valentim, L.M., Akbar, M.T., de Belleroche, J.S., Latchman, D.S., Gadian, D.G., 2005. Neuroprotective effects of HSP70 overexpression after cerebral ischaemia—an MRI study. Exp. Neurol. 195, 257–266.

Webster, C.M., Kelly, S., Koike, M.A., Chock, V.Y., Giffard, R.G., Yenari, M.A., 2009. Inflammation and NFkappaB activation is decreased by hypothermia following global cerebral ischemia. Neurobiol. Dis. 33, 301–312.

Wieloch, T., Miyauchi, Y., Lindvall, O., 1990. Neuronal damage in the striatum following forebrain ischemia: lack of effect of selective lesions of mesostriatal dopamine neurons. Exp. Brain Res. 83, 159–163.

Yenari, M.A., Fink, S.L., Sun, G.H., Chang, L.K., Patel, M.K., Kunis, D.M., Onley, D., Ho, D.Y., Sapolsky, R.M., Steinberg, G.K., 1998. Gene therapy with HSP72 is neuroprotective in rat models of stroke and epilepsy. Ann. Neurol. 44, 584–591.

Yi, J.J., Ehlers, M.D., 2005. Ubiquitin and protein turnover in synapse function. Neuron 47, 629–632.